ChemComm

COMMUNICATION

View Article Online
View Journal | View Issue



Cite this: *Chem. Commun.*, 2014, 50, 6630

Received 18th March 2014,
Accepted 2nd May 2014

DOI: 10.1039/c4cc02016b

www.rsc.org/chemcomm

# Electrocatalytic hydrogen generation by a trithiolato-bridged dimanganese hexacarbonyl anion with a turnover frequency exceeding 40 000 $s^{-1}$†

Kaipeng Hou, Hwa Tiong Poh and Wai Yip Fan*

**An unusual ionic manganese model complex $[Mn(bpy)_3]^+[(CO)_3Mn(\mu\text{-}SPh)_3Mn(CO)_3]^-$ (bpy: 2,2′-bipyridine) has been synthesized, which bears some structural resemblance to the active site of [FeFe] hydrogenase. An overpotential of 0.61 V has been determined for the electrocatalytic proton reduction using this complex in $CH_3CN$ with $CF_3COOH$ as the proton source. A turnover frequency of 44 600 $s^{-1}$ is achieved at high scan rates and in the presence of a large amount of acid.**

Hydrogenase enzymes are divided into three types according to the different metals in the active sites: [NiFe], [FeFe] and [Fe] only.[1] The former two can catalyze reversible proton reduction to molecular hydrogen at low overpotentials with remarkable efficiency.[2] In the [FeFe] hydrogenase, the two iron centres bearing CO and CN ligands are bridged by a unique azadithiolate ligand for which the nitrogen atom serves as the protonation site during proton reduction.[3] The reduction is assumed to be a $2e^-$ process where the 2Fe2S core provides one electron with the second electron supplied by the [Fe4S4] cluster (Scheme 1).[4]

There have been many studies on synthetic [FeFe] hydrogenase models based on the $\mu^2$-dithiolato-bridged diiron moiety $(\mu^2\text{-}RS)_2Fe_2$ coordinated to a variety of ligands such as CO, amines and phosphines. Several reviews have resulted from extensive studies on their structures, infrared spectroscopy and proton reduction efficiencies with acetic acid or trifluoroacetic acid as proton sources.[5–7] Recently, a Ni–Mn model complex has been synthesized whereby an azadiphosphine $(Ph_2P)_2NR$-chelated nickel center was linked to manganese by two thiolate ligands.[8] The Artero group introduced a dinuclear Ni–Mn complex as a bio-inspired mimic of the active site of [NiFe] hydrogenases catalyzing hydrogen evolution from trifluoroacetic acid with an overpotential 0.86 V.[9] Although many thiolate-bridged dimanganese complexes have been prepared, no studies on their proton reduction catalytic efficiencies have been reported. Furthermore the many different oxidation states exhibited by manganese should enable redox reactions to be carried out in a facile manner.

In this work, we will show that a $\mu_3$-thiolato dimanganese hexacarbonyl anion, $Mn_2(SPh)_3(CO)_6^-$ (complex **1** in Scheme 1), which structurally resembles the active site of [FeFe] hydrogenase, can catalyze electrochemical proton reduction with low overpotential coupled with very high turnover rates. We will also present a mechanism based on the experimental results.

Complex **1** is synthesized *via* a one-pot UV photolysis of $Mn_2(CO)_{10}$, diphenyl disulfide and 2,2′-bipyridine for 2 hours. An alternative pathway to **1** is also carried out whereby $Mn_2(CO)_{10}$ and diphenyl disulfide are UV-irradiated to first form the dithiolato-bridged complex $[Mn(CO)_4(\mu\text{-}SPh)]_2$. This complex is further irradiated in the presence of 2,2′-bipyridine to generate **1**. Suitable crystals of **1** are grown in acetone solvent and stored at low temperature before being subjected to X-ray diffraction.

Complex **1** consists of a dinuclear manganese anion and a mono-manganese cation (Fig. 1). The anionic part is $[(CO)_3Mn(\mu\text{-}SPh)_3Mn(CO)_3]^-$, which contains two manganese(I), each coordinated by three terminal CO ligands and bridged by three μ-SPh ligands. The phenyl groups are not coplanar due to steric repulsion but instead form a propeller-like arrangement. The distance between the two Mn atoms is 3.1646(10) Å which is too long for a Mn–Mn single bond.[10] The IR spectra of complex **1** show two strong $\nu_{CO}$ absorptions at 1910 and 1992 $cm^{-1}$ whose patterns are indicative of $C_{3v}$ symmetry around each of the Mn centre. The Mn(I) center in the $Mn(bpy)_3^+$ cation is coordinated by three bidentate bipyridine ligands, resulting in a highly-distorted octahedral geometry.

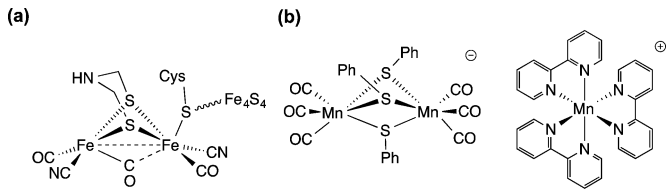


Scheme 1 (a) Active site of [FeFe] hydrogenase and (b) model complex **1** of this work.

*Department of Chemistry, National University of Singapore, 3 Science Drive 3, Singapore 117543, Singapore. E-mail: chmfanwy@nus.edu.sg*

† Electronic supplementary information (ESI) available. CCDC 991316. For ESI and crystallographic data in CIF or other electronic format see DOI: 10.1039/c4cc02016b

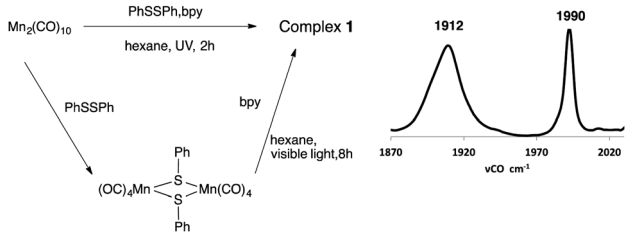


Fig. 1 Two pathways to form complex **1** and the $\nu_{CO}$ IR spectra of complex **1** in $CH_3CN$.

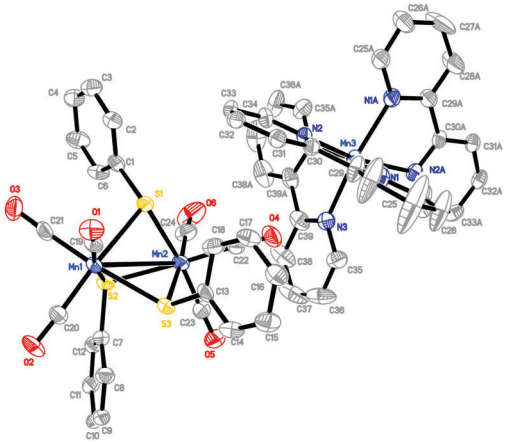

Fig. 2 ORTEP view of the solid-state structure of **1**. Hydrogen atoms are omitted for clarity.

The Mn–N bond lengths range from 2.236(4) to 2.263(4) Å, which are similar to those reported for Mn(II) octahedral tris(2,2′-bipyridine) complexes (Fig. 2).[11]

The route to the formation of **1** is complicated. Successive nucleophilic substitution of the $Mn_2(CO)_8(SPh)_2$ dimer by 2,2′-bipyridine will eventually afford $Mn(bpy)_3^+$ and $PhS^-$. The thiolate ion then reacts with the dimer to generate $Mn_2(CO)_3(SPh)_3^-$ upon dissociation of two Mn–CO bonds.

The cyclic voltammetric diagram of **1** in the absence of acid shows a small reduction peak at −1.90 V (*vs.* $Fc^+/Fc$ in $CH_3CN$), which corresponds to the reduction of the $Mn(bpy)_3^+$ cation respectively (Fig. 3). The assignment is based on a previous study on the reduction potentials of Mn(I) to Mn(0) bipyridine complexes.[12] As the addition of trifluoroacetic acid (TFA) causes the peak intensity to increase as well, it would appear that the cation itself is able to catalyze proton reduction albeit at a relatively high overpotential of 1.01 V (TFA reduction in $CH_3CN$ occurs at −0.89 V *vs.* $Fc^+/Fc$). Another smaller reduction peak is observed at −1.50 V, which we have attributed to the reduction of the anion. Interestingly this peak appears to have shifted to −1.20 V upon acid addition and remains at constant height independent of the acid concentration. We believe that protonation of the anion has taken place and hence reduces its reduction potential, as opposed to the higher charge repulsion between the anion and the electron in the absence of acid. At the same time a large peak which grows with the addition of acid is observed at −1.50 V to −1.60 V depending on the acid concentration.[8] The potential at −1.50 V is attributed to the catalytic proton

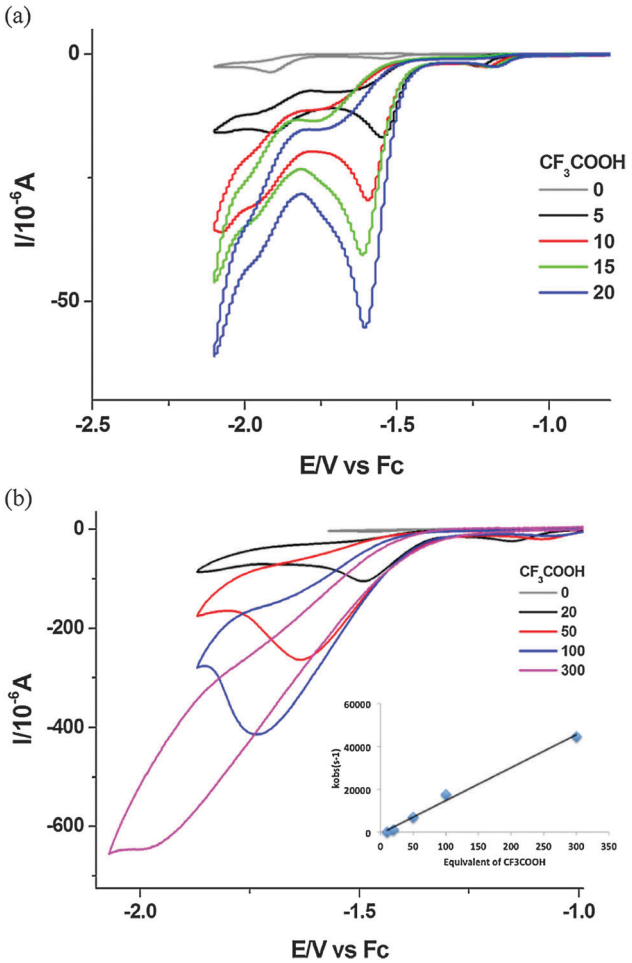


Fig. 3 (a) Cyclic voltammograms of **1** (1.0 mM) with TFA (0–20 mM) in 0.1 M $Bu_4NPF_6$ in $CH_3CN$ at a scan rate of 0.1 V $s^{-1}$. (b) Cyclic voltammograms of **1** (1.0 mM) with TFA (0–300 mM) in 0.1 M $Bu_4NPF_6$ in $CH_3CN$ at a scan rate of 1 V $s^{-1}$. The relationship of $k_{obs}$ with increasing acid concentration (inset graph). 1 mm glassy-carbon working electrode, platinum counter electrode at 295 K.

reduction potential of the anion, which corresponds to an overpotential of 0.61 V. The electrocatalytic $H_2$ production was further confirmed by bulk electrolysis of **1** with excessive $CF_3COOH$ in $CH_3CN$ at −1.50 V *vs.* $Fc^+/Fc$ with consistently more than 75% Faraday yield.

The catalytic rate of proton reduction is investigated next. To estimate the rate, an approximate model for pseudo-first-order catalytic systems previously used before is adopted here, as shown by the following equation.[13]

$$\frac{i_c}{i_p} = \frac{n}{0.446}\sqrt{\frac{RTk_{obs}}{F\upsilon}}$$

$i_c$ is the catalytic current, $i_p$ is the peak current measured in the absence of acid, $n$ is the number of electrons involved in the catalytic reaction, $k_{obs}$ is the observed first-order rate constant, $R$ is the ideal gas constant, $T$ is the temperature in Kelvin, $F$ is Faraday's constant, $\upsilon$ is the scan rate. From our data (Fig. 3b), it can be observed that $k_{obs}$ increases linearly with acid

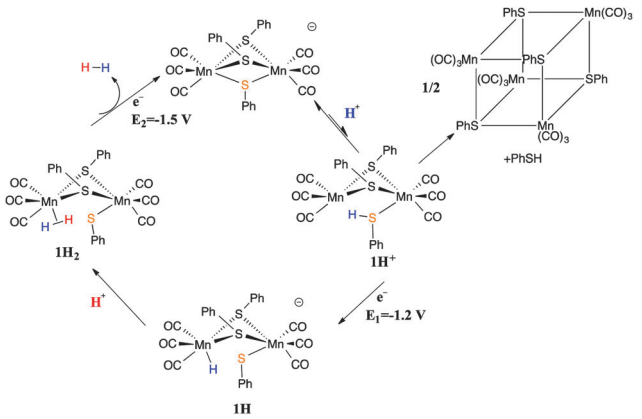


Fig. 4 Proposed mechanism for the proton reduction process based on experimental results.

concentration, which suggests a first-order dependence of the catalytic rate on acid concentration. At the highest concentration of $CF_3COOH$ (300 mM) studied, a $\frac{i_c}{i_p}$ value of 152 was obtained, which corresponds to a turnover frequency of 44 600 $s^{-1}$ at 295 K.

From the CV measurements, the anion appears to play a more important role in reducing the overpotential of proton reduction, hence the anion-catalysed mechanism is studied in more detail here. From the sequence of the process, the proton reduction mechanism catalyzed by **1** is proposed to be a CECE (chemical–electrochemical–chemical–electrochemical) process similar to that in iron and nickel model complexes (Fig. 4). The anion is first protonated to form intermediate $\mathbf{1H^+}$. Then $\mathbf{1H^+}$ is reduced at −1.2 V *vs.* $Fc^+$/Fc to generate a hydride species **1H** by an intrahydride transfer from sulfur to manganese.[14] A second proton reacts with **1H** to generate $\mathbf{1H_2}$. Finally, dihydrogen is released and the anion is regenerated upon electron reduction at −1.5 V *vs.* $Fc^+$/Fc to complete the catalytic cycle.

To gain more insight into the mechanism, the reactivity and stability of **1** in the presence of acids are first studied *via* infrared spectroscopy. When one equivalent $CF_3COOH$ is added to **1** in $CH_3CN$, no change in the $\nu_{CO}$ peaks is observed even after an hour. However, when the amount of acid is increased to 50 equivalents, the initial peaks of **1** at 1910 $cm^{-1}$ and 1992 $cm^{-1}$ slowly decrease while two new peaks at 1932 $cm^{-1}$ and 2015 $cm^{-1}$ appear. Based on a literature search, we were able to assign the 1932 and 2015 $cm^{-1}$ bands to the manganese carbonyl tetramer $Mn_4(CO)_{12}(SPh)_4$.[15]

The study indicates that **1** is moderately stable under acidic conditions, at least within the period when cyclic voltammetric studies were carried out. Hence the redox processes at different acid concentrations are due to **1** rather than the intermediates formed upon acidification. The tetrameric manganese cluster is probably formed from the dimerization of intermediate $\mathbf{1H^+}$ upon the dissociation of its benzenethiol ligand. Hence the tetramer formation may represent a competing reaction step for the reduction of intermediate $\mathbf{1H^+}$ to **1H**. However, our experimental data suggest that $\mathbf{1H^+}$ is relatively stable since the formation of the manganese tetramer is shown to be sluggish which in turn enables a high proton reduction catalytic rate to be achieved.

Although the overpotentials of many [FeFe] hydrogenase model complexes such as the diiron dithiolato bridged complexes fall within 0.2 V and 1.1 V, very few complexes actually exhibited overpotentials smaller than 0.6 V.[5] However complexes with low overpotentials are also less efficient in generating large proton reduction currents. The TOF for proton reduction catalysed by a diiron complex[16] can reach 58 000 $s^{-1}$ while the highest TOF reported for a nickel complex in dry and wet $CH_3CN$ were 33 000 $s^{-1}$ and 106 000 $s^{-1}$, respectively, with an overpotential of 0.625 V.[13,14] A comparison with these iron and nickel models shows that complex **1** is indeed a fairly efficient catalyst for proton reduction with an overpotential of 0.61 V. However if the homoconjugation effect of TFA is considered, the overpotential would become 0.79 V while Helm's method would give a value of 0.69 V.[17,18]

In summary, we have shown that a manganese complex, which is structurally similar to the active site of [FeFe] hydrogenase, can catalyze proton reduction with high TOF. The unusual structure of complex **1** contains a dinuclear manganese anion bridged by three μ-SPh groups and a mono-manganese cation where Mn(I) is coordinated by three 2,2′-bipyridine ligands. A simple mechanism showing how proton reduction takes place electrochemically is also proposed. We have demonstrated that the manganese-only model complex can also catalyze proton reduction at least as efficient as some iron or nickel model complexes.

The authors are grateful for a NUS research grant (143-000-553-112).

## Notes and references

1 D. J. Evans and C. J. Pickett, *Chem. Soc. Rev.*, 2003, **32**, 268.
2 A. L. De Lacey, V. M. Fernández, M. Rousset and R. Cammack, *Chem. Rev.*, 2007, **107**, 4304.
3 A. M. Appel, J. E. Bercaw, A. B. Bocarsly, H. Dobbek, D. L. DuBois, M. Dupuis, J. G. Ferry, E. Fujita, R. Hille and P. J. A. Kenis, *Chem. Rev.*, 2013, **113**, 6621.
4 F. Gloaguen and T. B. Rauchfuss, *Chem. Soc. Rev.*, 2009, **38**, 100.
5 G. A. N. Felton, C. A. Mebi, B. J. Petro, A. K. Vannucci, D. H. Evans, R. S. Glass and D. L. Lichtenberger, *J. Organomet. Chem.*, 2009, **694**, 2681.
6 J.-F. Capon, F. Gloaguen, F. Y. Pétillon, P. Schollhammer and J. Talarmin, *Coord. Chem. Rev.*, 2009, **253**, 1476.
7 C. Tard and C. J. Pickett, *Chem. Rev.*, 2009, **109**, 2245.
8 L.-C. Song, J.-P. Li, Z.-J. Xie and H.-B. Song, *Inorg. Chem.*, 2013, **52**, 11618.
9 V. Fourmond, S. Canaguier, B. Golly, M. J. Field, M. Fontecave and V. Artero, *Energy Environ. Sci.*, 2011, **4**, 2417.
10 J. W. McDonald, *Inorg. Chem.*, 1985, **24**, 1734.
11 X.-L. Yu, Y.-X. Tong, X.-M. Chen and T. C. W. Mak, *J. Chem. Crystallogr.*, 1997, **27**, 441.
12 M. Wang, J. England, T. Weyhermüller and K. Wieghardt, *Inorg. Chem.*, 2014, **53**, 2276.
13 M. L. Helm, M. P. Stewart, R. M. Bullock, M. R. DuBois and D. L. DuBois, *Science*, 2011, **333**, 863.
14 M. Dupuis, S. Chen, S. Raugei, D. L. DuBois and R. M. Bullock, *J. Phys. Chem. A*, 2011, **115**, 4861.
15 M. Reyes-Lezama, R. A. Toscano and N. Zuñiga-Villareal, *J. Organomet. Chem.*, 1996, **517**, 19.
16 M. E. Carroll, B. E. Barton, T. B. Rauchfuss and P. J. Carroll, *J. Am. Chem. Soc.*, 2012, **134**, 18843.
17 V. Fourmond, P.-A. Jacques, M. Fontecave and V. Artero, *Inorg. Chem.*, 2010, **49**, 10338.
18 A. M. Appel and M. L. Helm, *ACS Catal.*, 2014, **4**, 630.

 